AD-A140 615 DISTRIBUTIONS OF AURORA AND IONOSPHERIC CURRENTS OBSERVED SIMULTANEOUSLY O..(U) IOWA UNIV IOWA CITY DEPT OF PHYSICS AND ASTRONOMY J D CRAVEN ET AL. AUG 83 1/1

UNCLASSIFIED U. OF IOWA-83-26 N00014-76-C-0016 F/G 4/1 NL

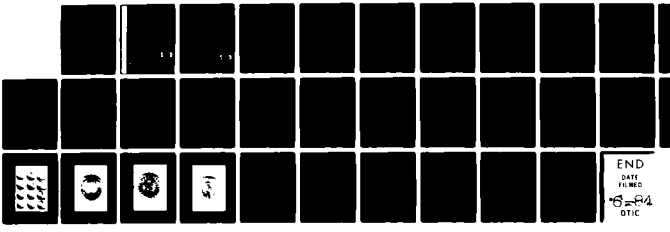

END
DATE FILMED
6-84
DTIC

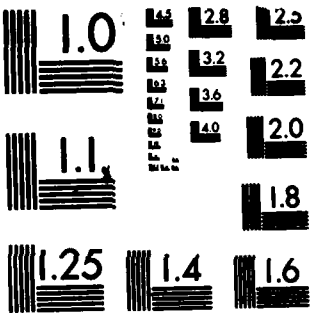

MICROCOPY RESOLUTION TEST CHART
NATIONAL BUREAU OF STANDARDS-1963-A

10

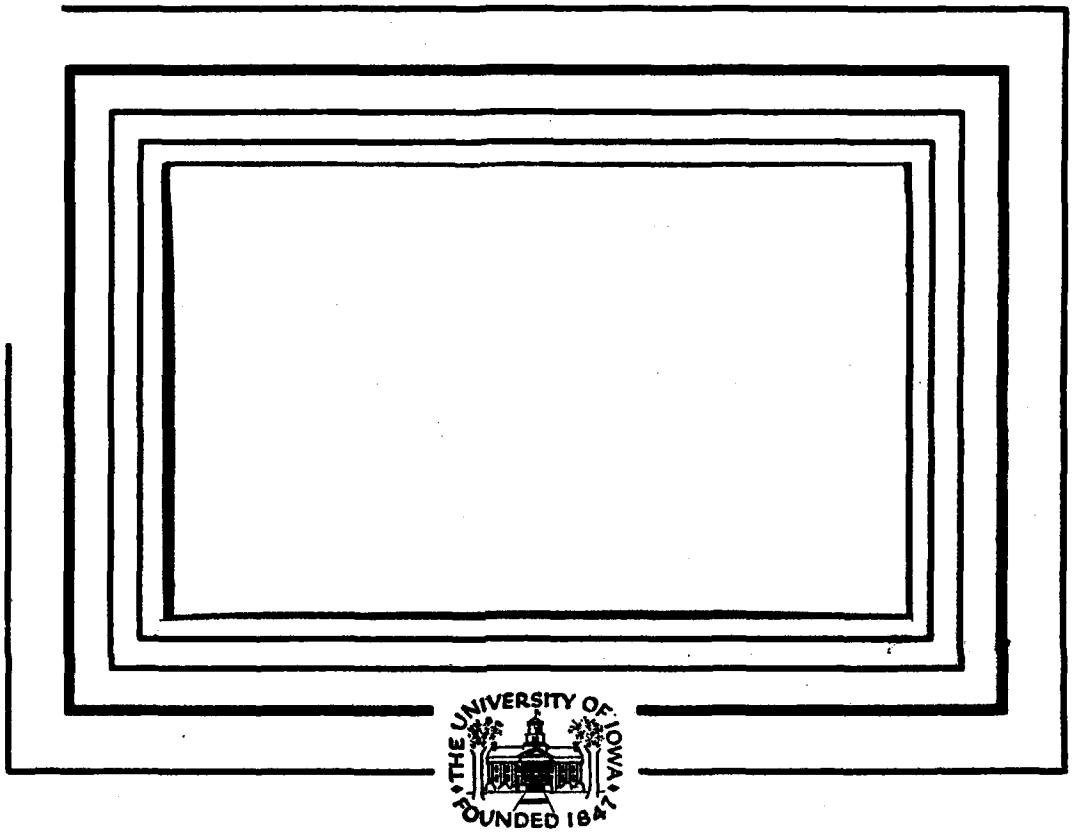

Department of Physics and Astronomy

THE UNIVERSITY OF IOWA

Iowa City, Iowa 52242

U. of Iowa 83-26

DISTRIBUTIONS OF AURORA AND IONOSPHERIC CURRENTS OBSERVED SIMULTANEOUSLY ON A GLOBAL SCALE

by

J. D. Craven[1], Y. Kamide[2], L. A. Frank[1],

S.-I. Akasofu[3] and M. Sugiura[4]

[1]Department of Physics and Astronomy
The University of Iowa, Iowa City, Iowa 52242

[2]Kyoto Sangyo University
Kamigamo, Kita-ku
Kyoto 603, Japan

[3]Geophysical Institute
The University of Alaska, Fairbanks, Alaska 99701

[4]Laboratory for Extraterrestrial Physics
Goddard Space Flight Center
Greenbelt, Maryland 20771

August 1983

Department of Physics and Astronomy
The University of Iowa
Iowa City, Iowa 52242

To be published in Magnetospheric Currents,
AGU Geophysical Monograph #28

Abstract

The instantaneous spatial distribution of auroral emissions is observed with auroral imaging photometers on board the spacecraft Dynamics Explorer 1 (DE 1) as ground-based meridian chains of magnetometers simultaneously detect the magnetic signatures of ionospheric and field-aligned currents flowing at northern polar latitudes. Ionospheric conductivities at nighttime auroral latitudes are estimated from the measured auroral luminosities and used with the measured polar magnetic variations to compute model distributions of ionospheric and field-aligned currents. Temporal resolution for the coordinated observations and model calculations is 12 minutes. Model ionospheric and field-aligned current distributions are overlayed on global auroral images to illustrate spatial relations on a global scale at the maximum epoch of an auroral substorm. Eccentric-dipole-latitude and magnetic-local-time coordinates are used. A model field-aligned current distribution is compared quantitatively with the distribution of field-aligned currents inferred from simultaneous observations by the DE-2 magnetometer.

Introduction

A small number of meteorological spacecraft are able to monitor significant portions of the terrestrial atmosphere on a continuous basis through the use of remote-sensing instrumentation at visible and infrared wavelengths. When combined with local and remote observations gained by a distribution of ground- and aircraft-based instruments, an extensive data base is available for investigations of atmospheric dynamics on a global scale. A similar capability does not exist in magnetospheric studies as significant portions of the magnetosphere can not be sampled by remote-sensing instruments and because the fiscal and technical requirements would be immense to install and operate a widely distributed spacecraft network within and about the extensive magnetospheric cavity. A program less comprehensive than that in meteorology is in place, however. The magnetosphere is sampled routinely by a small number of earth-orbiting spacecraft (e.g., IMP 8; ISEE 1,2; Dynamics Explorer 1) through measurements of local plasma and plasma-wave environments, and of local electric and magnetic fields. Distant plasma-wave source regions are identified by direction finding techniques and images of the aurora are gained at visible and ultraviolet wavelengths. Remote sensing of the aurora on a global scale provides direct observations of the inner boundary of the magnetospheric system at the ionosphere. Below this interface at ground level widely distributed observations are (or can be) made to monitor physical parameters of that boundary (e.g., electron densities, drift speeds, ionospheric currents and auroral emissions).

The geometric configuration of the near-earth magnetosphere is determined primarily by the earth's magnetic field while the configuration of the more distant magnetosphere is determined in large part by current systems established in response to the incident solar-wind plasma and the induced electric field. A principal objective of magnetospheric physics is the identification of these current systems and their responses to variations in the interplanetary environment. Surprisingly, gross current patterns within the distant magnetosphere identified to date are largely inferred from the magnetic field configuration, and not from direct measurements of the current carriers. Recent new measurements within the distant magnetosphere [Frank et al., 1983] provide direct observations of these currents.

At much lower altitudes (typically $\lesssim 4$ R_E) magnetically field-aligned currents are routinely identified at high latitudes by direct detection of the charge carriers and indirectly by means of magnetometers [e.g., Sugiura et al., 1983]. The principal charge carriers for outwardly directed currents appear to be the energetic electrons responsible for auroral optical radiation and enhanced ionization within the ionosphere. Typical energies vary from hundreds of electronvolts to tens of kiloelectronvolts. Direct detection of charge carriers responsible for the inwardly directed currents continues to challenge investigators. The spatial distributions of ionospheric electric fields and the enhanced ionospheric conductivities direct ionospheric currents along and across the auroral regions. At ground level the horizontal component of this current (the auroral electrojet) is readily detected by its magnetic signature. Ground level detection of magnetic fields arising from magnetically field-aligned closure currents to and from the distant magnetosphere is more difficult. Recently developed advanced computer codes make possible the approximate determination of the large-scale distributions of these field-aligned currents [Akasofu et al., 1981].

Analysis of ground-based and low-altitude spacecraft observations provided the early average global views of the high-latitude regions. The distributions of magnetic perturbations from the auroral electrojets [Silsbee and Vestine, 1942; Harang, 1946], of the optical aurora [Feldstein, 1963] and of field-aligned currents above the auroral zones [Zmuda and Armstrong, 1974] demonstrate the presence of intense current systems with a complex continuity in local time and a confinement to a small range of latitudes generally referred to as the auroral latitudes. Imaging instrumentation on board the ISIS-2 and DMSP spacecraft have confirmed the complex distributions of auroral emissions in local time at visible and near-infrared wavelengths by providing views of significant portions of the auroral zones [e.g., Anger et al., 1973; Snyder et al., 1974] and of the full auroral region [Murphree and Anger, 1980]. Orbital periods of ~ 100 minutes determine the basic temporal resolution for observations with these optical instruments. This time interval is long in comparison to time scales for most temporal variations in auroral phenomena.

A dynamical description of auroral phenomena on a global scale was developed in the early 1960's from the extensive library of all-sky auroral photographs obtained during the International Geophysical Year [Akasofu, 1964]. While the initial models were based upon collections of observations, each covering a small portion of the auroral region, more refined later models have been based upon individual DMSP and ISIS-2 images of significant fractions of the auroral regions. Photo-mosaics of all-sky and DMSP photographs are used frequently to illustrate the several stages of auroral activity in the substorm model [see Chapter 2 of Akasofu, 1977].

Dynamics of the auroral electrojet current systems have been investigated with chains of magnetometers distributed in latitude along magnetic meridians [e.g., Kisabeth, 1979]. The six meridian chains of more than 70 magnetometers assembled for the International Magnetospheric Study (IMS) represent the most comprehensive investigation from the ground to date of auroral magnetic phenomena. Kamide et al. [1982] have developed computer algorithms which use these extensive observations to determine ionospheric electric fields, currents and Joule-heating rates, and the magnitudes of field-aligned currents towards and away from the ionosphere. Temporal resolutions of several minutes are obtained by Kamide and coworkers.

This greatly increased temporal resolution exceeds that of nearly all other available global magnetospheric observations, but effective utilization has been hampered in part by the lack of simultaneous determinations of ionospheric conductivities with comparable temporal resolution. What have been used are conductivity distributions based upon average particle precipitation patterns as a function of magnetic activity. The application of these average conductivity models in the algorithim of Kamide et al. [1981] is discussed by Kamide et al. [1982]. Conductivities arising from ultraviolet insolation are calculated for standard model upper atmospheres.

With the launch of the spacecraft Dynamics Explorer 1 in August 1981 [Hoffman et al., 1981] global auroral imaging has become available at visible and ultraviolet wavelengths with temporal resolutions of 12 minutes [Frank et al., 1981]. This ability to determine the distributions of auroral emissions with good spatial and temporal resolution at three wavelengths, simultaneously, provides a unique opportunity to obtain improved ionospheric conductivities on a global scale. Additionally, auroral imaging provides

indirect observations of field-aligned currents directed out of the ionosphere at auroral and polar-cap latitudes due to precipitating auroral electrons.

The availability of accurate models for the instantaneous ionospheric and field-aligned current systems at the ionospheric boundary of the magnetosphere can provide an additional, significant tool for studies of the dynamics of magnetospheric current systems. Several correlative investigations outlined in Figure 1 are being developed, with the triad of investigations using ground and near-earth observations the subject of this paper.

Observations

For this investigation magnetic records are presently available from 34 ground magnetometer stations. These stations are identified in Table 1 and their eccentric-dipole coordinates [Cole, 1963] tabulated. The spatial distribution of the stations in an eccentric-dipole-latitude, magnetic-local-time format is illustrated in Figure 2 to identify those portions of the polar region for which ground observations are available. The local-time distribution is given for 0610 UT. Good spatial coverage is available from the magnetic pole to ~ 65° latitude over a 12-hour interval of local time, and then to ~ 55° latitude over a 6-hour interval, each centered near local midnight. In each case the largest concentration of stations is found at the earlier local times. The Scandinavian chain of stations is located at approximately 0800 hours local time.

Magnetic records from analog-recording stations are digitized at the University of Alaska's Geophysical Institute and combined with digitally recorded data to provide a data base of magnetic perturbation vectors referenced to quiet auroral conditions with one minute temporal resolution. These data are used by Kamide et al. [1981] to compute model ionospheric and field-aligned current systems. The perturbation vectors are also used to compute the auroral electrojet index AE(34) with which magnetic substorm activity is characterized on a global scale.

Optical images of the northern polar region are gained simultaneously at visible and ultraviolet wavelengths with auroral imaging instrumentation carried on the polar-orbiting spacecraft Dynamics Explorer 1 [Frank et al., 1981]. A combination of high apogee altitude (3.65 R_E) and an initial apogee latitude near 90° provides up to 5 hours of continuous auroral imaging for

each 6.83-hour orbit. By means of a method described by Kamide et al. [1983] these auroral images can be used to infer height-integrated ionospheric conductivities over the entire polar region with 12-minute time resolution.

Ionospheric Currents

Ionospheric currents are computed for an intense auroral substorm with an onset time of ~ 0700 UT on 8 November 1981. The AE index is ~ 220 nT at the onset and increases to ~ 1000 nT by the maximum epoch of the substorm at ~ 0850 UT. A steady decrease in the AE index follows, reaching ~ 150 nT by ~ 1020 UT.

Global auroral activity during this magnetic substorm displays a corresponding increase to maximum intensities by ~ 0850 UT, followed by decreases in the following hour. This temporal behavior is displayed in Plate 1 by a sequence of 12 consecutive auroral images in false color spanning the time interval 0719 to 0945 UT. The first image at upper left in the plate presents the spacecraft view of earth from 69° north latitude in the early-morning sector. With time the spacecraft proceeds from apogee inbound across the north pole (fifth frame at 0807 UT) and into the mid-evening sector. The universal time (UT) assigned to an image identifies the time at which the 12-minute image period begins. For this sequence each 30° X 30° nadir-centered image is a record of the emission intensities of ultraviolet light observed at wavelengths 120 to 155 nm. The geocorona is visible in the scattered light of solar Lyman-α radiation at upper left in the images, sunward of the dayside limb. Antisunward of the terminator the entire auroral region is detected, principally in the light of neutral atomic oxygen at 130.4 and 135.6 nm.

Acquisition of the first frame in the plate is initiated at 0719 UT as magnetic activity is just beginning to increase. The AE index is ~ 240 nT. By the fifth frame at 0807 UT the AE index exceeds 600 nT, and is ~ 1000 nT by the maximum epoch of the substorm at ~ 0850 UT (eighth frame). Throughout this interval auroral emissions increase steadily in brightness and latitudinal width. There is a marked poleward displacement at local midnight during the maximum epoch of the substorm. Images at 0856, 0908 and 0920 UT (ninth through eleventh frames) reveal that during the declining phase of magnetic activity a discrete arc along the nightside edge of the polar cap is replaced by a diffuse band of emissions. A system of discrete arcs reappers at 0932 UT (twelfth frame). Diffuse aurora are visible at more equatorward latitudes throughout the period.

Height-integrated conductivities are inferred from these auroral images in the manner described by Kamide et al. [1983]. A smoothed Pedersen conductivity distribution for this substorm at maximum epoch (0844 - 0856 UT) is shown in Plate 2 superposed over the original auroral image which is displayed in a false-color format. Light blue denotes emission intensities of ~ 2 kR, with greater intensities coded by green, yellow, red and white ($\gtrsim$ 32 kR). The conductivity distribution and auroral image are presented in eccentric-dipole-latitude, magnetic-local-time coordinates. A latitude of 50° is identified by the outer circle and concentric circles of smaller radii denote latitudes of 60°, 70° and 80°. The maximum conductivity of ~ 32 mhos is located at ~ 63° latitude and ~ 0100 hours local time. Hall conductivities are assumed to be twice the Pedersen conductivities. Magnetic perturbation

vectors for the 12-minute interval are obtained for each of the 34 ground stations by averaging the 12 samples obtained the 0844 to 0856 UT time interval. A model ionospheric current system is derived with the computer algorithm of Kamide et al. [1981] using the inferred conductivity distribution and the 34 magnetic perturbation vectors. This current system is displayed in Plate 3 using the format of Plate 2. Recalling the spatial distribution of ground stations illustrated in Figure 1 for 0610 UT, the 12-hour range of local times to 65° latitude and the 6-hour range to 55° are centered near 0230 hours local time. Within this 12-hour local time sector the latitude of maximum model westward electrojet current decreases monotonically from 69° eccentric dipole latitude at ~ 0830 hours local time to 66° at ~ 2030 hours local time. The latitude of maximum current lies near the poleward edge of maximum auroral intensities associated with the diffuse aurora (excluding the local enhancement in intensities at ~ 0030 hours and 69°). Width of the westward electrojet decreases from $\gtrsim$ 10° in the morning sector to ~ 5° in the late-evening sector. Maximum ionospheric currents range from 1.1 A/m at 0600 hours to 0.75 A/m at 2200 hours local time. A second westward electrojet near local midnight and ~ 76° is coincident with the most poleward arc of the expanding auroral bulge. A weak eastward electrojet is computed near local midnight and equatorward of ~ 60°. Westward currents in the morning sector at latitudes below 60° are coincident with aurora of intensities less than the 2-kR threshold used in displaying the image.

Field-Aligned Currents

A model field-aligned current distribution is obtained by computing the divergence of the ionospheric current distribution. The field-aligned current distribution for maximum epoch in the substorm is presented in Plate 4. The format is identical to that used for the two previous plates. The most striking features of this current distribution are the numerous cells of inwardly (solid lines) and outwardly (dashed lines) directed currents concentrated within the polar cap. Maximum current densities are ~ 1.5 $\mu A/m^2$. No aurora of intensities greater than ~ 1 kR are detected within the polar cap which can be associated with these model cells of field-aligned currents.

At the latitudes of maximum intensities in the diffuse aurora the predominant feature of the model current system is a ~ 5° - 8° wide distribution of outwardly directed currents with typical densities ~ 0.6 $\mu A/m^2$ in the pre-midnight and post-dawn local-time sectors. These distributions are coincident in latitude with the diffuse aurora but are not coincident in local time with the locations of maximum auroral intensities. The minimum current density contour in this plate is 0.3 $\mu A/m^2$. The current distribution for the previous 12-minute interval, with a minimum current density contour of 0.1 $\mu A/m^2$, demonstrates more clearly that outward currents in excess of 0.2 $\mu A/m^2$ are present at latitudes 60° - 70° over a large range of local times. Within the 0000 to 0300 hour local time sector inward currents of the order of 0.2 $\mu A/m^2$ are computed for these latitudes. This current distribution is a low-latitude extension to earlier local times of a more intense model current distribution centered at 71° and 0500 hours. In the morning sector the distributions of outward currents are displaced equatorward of the westward electrojet by ~ 3 degrees, and are nearly coincident in the late-evening sector.

Comparison with DE-2 Observations

Further analysis of the model field-aligned current distributions is gained through comparisons with simultaneous observations from low-altitude spacecraft magnetometers. An example of available simultaneous observations is found in the interval from 0603 to 0619 UT on 7 November 1981 when the DE-2 spacecraft passed over the IMS Scandinavian magnetometer chain, proceeded across the polar cap and then crossed over Alaska. A mapping of this portion of the DE-2 orbit along the magnetic field to an altitude of 100 km is displayed in Figure 2. Local times for this spatial distribution of ground magnetometers and the orbit mapping are determined for 0610 UT, when the spacecraft is traversing the polar-cap region midway between auroral zone crossings at 0800 and 1800 hours local time. An auroral substorm occurring in the period 0440 - 0600 UT has been discussed previously by Kamide et al. [1983]. The DE-2 polar crossing occurs at the end of this substorm as a system of intense arcs is brightening in the evening sector and advancing poleward. Auroral intensities in the morning sector near 0800 hours local time remain diffuse and weak by comparison (see Plate 1 of Kamide et al., [1983]).

Summaries of the observations with the DE-2 magnetometer, the 34 ground magnetometers and the DE-1 auroral imaging instrumentation are presented in Figures 3 and 4. Observations in the morning (evening) sector are presented in Figures 3 (4). Observed deviations of the horizontal component of the geomagnetic field perpendicular to the DE-2 orbit plane are shown in the upper panel of each figure. Smaller deviations parallel to the orbit plane are ignored in this analysis. Assuming a distribution of infinite field-aligned current sheets tangential to the geomagnetic dipole L shells, current

distributions are computed from the observed magnetic perturbations. The magnitudes and directions of these computed current distributions are shown in the second panel of each figure. Current directions are specified with respect to the ionosphere. The magnetic perturbations and inferred current densities are plotted as functions of time. Eccentric dipole latitudes at significant locations are mapped from the abscissas by dashed lines.

Simultaneously with the DE-2 crossings of the auroral field lines in the morning and then the evening sectors, the DE-1 auroral imagers measured auroral emission intensities at the ionospheric intersections of the DE-2 magnetic field lines. A slant angle of ~ 40° and a large radial distance to the weaker morning-side aurora results in separations of ~ 1° in latitude between consecutive pixels in an image scan line. In the evening sector the separations are ~ 0.4°. The auroral luminosities are plotted in the lower panel of each figure. The errors in determining the geographic and then geomagnetic coordinates of a pixel are less than the angular width of a pixel.

Model field-aligned current distributions hve been determined from ground magnetometer observations in the time intervals 0605 - 0607 UT and 0616 - 0618 UT for concurrent observations with the DE spacecraft in the morning and evening sectors, respectively. From the resulting current density contours of the form illustrated in Plate 4, current densities are determined along the DE-2 orbit track. These current-density profiles are presented in the third panels of the two figures. Ground magnetometer stations near the DE-2 ground track are identified by number from Table 1.

In the morning sector (Figure 3), field-aligned currents with densities in excess of ~ 1 $\mu A/m^2$ are detected with DE-2 at latitudes 69° to 72.6°. The lowest latitude current sheet is located at 69°, with current densities of 6-8 $\mu A/m^2$ directed out of the ionosphere. Poleward at 69.5° and 71° inward currents with peak current densities of 10 and 8 $\mu A/m^2$ are detected. In the evening sector (Figure 4) an upward current is located at the poleward edge of the auroral zone coincident with greatly increased optical emissions of ~ 6 kR. An untimely data gap prohibits accurate computation of currents densities equatorward of this intense (~ 9 $\mu A/m^2$) outward current, but the magnetic perturbations on either side of the data gap establish the presence of an inward current equatorward of the outward current. Multiple current sheets with smaller densities are observed at more equatorward latitudes. The spatial distribution in the morning (evening) sector of inward (outward) currents is in agreement with previous spacecraft observations [e.g., Iijima and Potemra, 1976].

This direct comparison with spacecraft observations illustrates clearly a difficulty inherent in models of global field-aligned current distributions which are based upon a widely spaced distribution of ground magnetometers: the field-aligned current sheets have latitudinal widths and separation distances which are small compared to the resolutions provided by the distributions of ground magnetometers and the computational schemes. These modeled current distributions may provide smoothed, average values for the large scale features, but cannot resolve the observed multiple current sheets with adjacent, oppositely directed currents.

In the evening sector (Figure 4) four ground stations are located at latitudes for which 1-2 $\mu A/m^2$ field-aligned current densities are detected with DE 2. The most poleward station (Barrow, #16) is located ~ 1.5° equatorward of the intense upward current sheet at ~ 73° for which the current sheet intensity is ~ 0.3 A/m, and ~ 1° from the inferred downward current sheet for which the estimated current sheet intensity is ~ 0.1 A/m. These current sheets provide a net upward current intensity of ~ 0.2 A/m which is the principal source of field-aligned currents near the Barrow ground station. The current sheet intensity computed from the model current densities at latitudes 70° - 73° is ~ 0.1 A/m, upward, in reasonable agreement with the DE-2 observation, but the sheet is located ~ 1.5° equatorward of the current sheets observed with DE 2. The absence of a ground station poleward of 73° precludes improved spatial agreement. The large inwardly directed currents poleward of 73° are nonphysical artifacts of the model solution.

In the morning sector (Figure 3) only one ground station (Bjornoya, #18) is located within the latitudinal range of significant field-aligned currents. Intensities of the four principal current sheets nearest the ground station are approximately 0.3 A/m outward and 0.2 A/m inward at ~ 69.2° and 0.15 A/m inward and 0.05 A/m outward at ~ 70.6°. The net current intensities at the two latitudes are approximately 0.1 A/m outward and 0.1 A/m inward, respectively. The magnitudes of the current sheet intensities computed by the model for outward currents (57° -67°) and inward currents (67° - 77°) are each ~ 0.1 A/m. While these values for average current sheet intensities compare favorably with the observed values, a comparison of the spatial distributions indicates little agreement.

Conclusions

Determination of the simultaneous distributions of the aurora and ionospheric currents on a global scale as a function of time with good temporal resolution will provide a new tool for studies of magnetospheric current systems. The auroral images provide a means of obtaining improved conductivity models for polar latitudes which can be used with advanced computer codes to obtain the distributions of ionospheric and field-aligned currents. The images also provide an indirect monitor of currents carried by precipitating auroral electrons.

Spatial resolutions with the network of ground magnetometers and the computational schemes are too coarse to resolve discrete, multiple current sheets present at auroral latitudes. These discrete current structures are observed only by in situ spacecraft observations. However, such observations reveal only local conditions at one instant in time, while the objective is to develop global-scale dynamic models which describe the average current systems at the magnetosphere's ionospheric boundary [e.g., Harel et al., 1981]. These models are a necessary part of the larger goal to obtain comprehensive dynamic models for the magnetospheric current systems. The in situ spacecraft observations are important to the development of these models by determining absolute magnitudes and latitudinal distributions of current sheet intensities whose averages should be described correctly by the models. The comparisons with DE-2 observations presented here demonstrate that the average sheet intensities can be obtained with the models. The latitudinal widths are comparable to the statistically determined distributions [e.g., Iijima and

Potemra, 1976]. Further improvements to the mathematical models may require the a posteriori inclusion of multiple current sheets. Correlative investigations with the two DE spacecraft of the spatial distributions of current sheets and aurora can provide necessary new information.

Large-scale current structures appear to be resolved with the present distribution of ground stations. Typical latitudinal widths for the auroral electrojets are comparable or greater than the differences in latitude between many adjacent ground stations. The electrojet's great extent in longitude and slow variation in latitude with local time further improve the determination of average magnitude, width and latitude. For the example provided in Plate 2 at maximum epoch in the substorm, the auroral electrojet follows the poleward edge of the diffuse aurora for the entire 12-hour local time interval covered by ground stations. Resolution is adequate to identify an electrojet at the poleward edge of the expanding auroral bulge approximately 10° poleward of the diffuse aurora.

Large-scale current structures of the polar cap should also be resolved, in particular during periods of enhanced auroral activity when discrete polar-cap aurora are not present. Present difficulties include polar-cap conductivity models, the smaller current densities of the polar-cap current systems and nonphysical model solutions in areas not adequately sampled by ground stations.

Acknowledgements

This research was supported at the University of Iowa in part by the National Aeronautics and Space Administration under contract NAS5-25689 and grant NGL 16-001-002 and by the Office of Naval Research under grant N00014-76-C-0016. Contributions to this research by the University of Alaska were supported by the National Science Foundation under grant ATM81.

References

Akasofu, S. -I., The development of the auroral substorm, Planet. Space Sci., 12, 273, 1964.

Akasofu, S. -I., Physics of Magnetospheric Substorms, D. Reidel, Dordrecht, Netherlands, 1977.

Akasofu, S. -I., Y. Kamide and J. Kisabeth, Comparison of two modeling methods for three-dimensional current systems, J. Geophys. Res., 86, 3389, 1981.

Anger, C. D., A. T. Y. Lui and S. -I. Akasofu, Observations of the auroral oval and a westward traveling surge from the Isis 2 satellite and the Alaskan meridian all-sky cameras, J. Geophys. Res., 78, 3020, 1973.

Cole, K. D., Eccentric dipole coordinates, Australian J. Phys., 16, 423, 1963.

Feldstein, Y. I., Some problems concerning the morphology of auroras and magnetic disturbances at high latitudes, Geomagn. Aeron., 3, 183, 1963.

Frank, L. A., J. D. Craven, K. L. Ackerson, M. R. English, R. H. Eather and R. L. Carovillano, Global auroral imaging instrumentation for the Dynamics Explorer mission, Sp. Sci. Instr., 5, 369, 1981.

Frank, L. A., C. Y Huang and T. E. Eastman, Currents in the earth's magnetotail, in Magnetospheric Currents, ed. by T. A. Potemra, AGU Geophysical Monograph #28, 1983.

Harang, L., The mean field of disturbance of polar geomagnetic storms, Terr. Magn. Atmos. Elec., 51, 353, 1946.

Harel, M., R. A. Wolf, P. H. Reiff, R. W. Spiro, W. J. Burke, F. J. Rich and M. Smiddy, Quantitative simulation of a magnetospheric substorm, 1. model logic and overview, J. Geophys. Res., 86, 2217, 1981.

Hoffman, R. A., G. D. Hogan and R. C. Maehl, Dynamics Explorer spacecraft and ground operations system, Sp. Sci. Instr., 5, 349, 1981.

Iijima, T., and T. A. Potemra, The amplitude distribution of field-aligned currents at northern high latitudes observed by TRIAD, J. Geophys. Res., 81, 2165, 1976.

Kamide, Y., A. D. Richmond and S. Matsushita, Estimation of ionospheric electric fields, ionospheric currents and field-aligned currents from ground magnetic records, J. Geophys. Res., 86, 801, 1981.

Kamide, Y., B. -H., Ahn, S. -I. Akasofu, W. Baumjohann, E. Friis-Christensen, H. W. Kroehl, H. Maurer, A. D. Richmond, G. Rostoker, R. W. Spiro, J. K. Walker and A. N. Zaitzev, Global distribution of ionospheric and field-aligned currents during substorms as determined from six IMS meridian chains of magnetometers: initial results, J. Geophys. Res., 87, 8228, 1982.

Kamide, Y, J. D. Craven, L. A. Frank and S. -I. Akasofu, Modeling substorm current systems using conductivity distributions inferred from DE auroral images, Geophys. Res. Lett.,(to be submitted), 1983.

Kisabeth, J. L., On calculating magnetic and vector potential fields due to large-scale magnetospheric current systems and induced currents in a infinitely conducting earth, in Quantitative Modeling of Magnetospheric Processes, ed. by W. P. Olson, AGU Geophysical Monograph 21, pp. 473, 1979.

Murphee, J. S. and C. D. Anger, An observation of the instantaneous optical auroral distribution, Can. J. Phys., 58, 214, 1980.

Silsbee, H. C., and E. H. Vestine, Geomagnetic bays, their frequency and current systems, Terr. Magn. Atmosph. Elect., 47, 195, 1942.

Snyder, A. L., S. -I. Akasofu and T. N. Davis, Auroral substorms observed from above the North Pole region by a satellite, J. Geophys. Res., 79, 1393, 1974.

Sugiura, M., T. Iyemori, R. A. Hoffman, N. C. Maynard, J. L. Burch and J. D. Winningham, Relationships between field-aligned currents, electric fields, and particle precipitation as observed by Dynamics Explorer-2, in Magnetospheric Currents, ed. by T. A. Potemra, AGU Geophysical Monograph #28, 1983.

Zmuda, A. J. and J. C. Armstrong, The diurnal flow pattern of field-aligned currents, J. Geophys. Res., 79, 4611, 1974.

Table 1. Eccentric-Dipole Coordinates of the Ground Magnetometers

No.	Station Name	Longitude	Co-Latitude
1	Resolute Bay	311.52	6.70
2	Yellowknife	294.13	20.38
3	Fort Churchill	323.00	22.47
4	Great Whale River	344.79	25.74
5	Cambridge Bay	301.74	12.96
6	Baker Lake	318.76	17.07
7	Meanook	299.66	28.07
8	St. John's	13.97	34.64
9	Ottawa	347.05	35.41
10	Mould Bay	262.58	8.27
11	Victoria	289.96	35.32
12	Alert	101.04	3.53
13	Glenlea	320.80	31.75
14	Igloolik	340.49	11.68
15	Tromso	98.44	24.12
16	Barrow	236.07	18.35
17	Ny Alesund	107.29	15.18
18	Bjornoya	104.11	19.80
19	Thule	22.55	4.54
20	Odessa	96.98	47.61
21	Leirvogur	56.90	22.97
22	Narssarssuaq	27.93	22.58
23	Cape Chelyuskin	159.85	21.62
24	Cape Wellen	230.37	25.17
25	Leningrad	101.57	34.96
26	Godhavn	25.46	13.78
27	Newport	297.26	34.75
28	Sachs Harbor	268.04	12.74
29	Norman Wells	276.32	19.21
30	Fort Simpson	286.19	21.97
31	Inuvik	264.86	17.34
32	Fort Yukon	253.82	20.83
33	Fort Smith	298.88	22.58
34	College	252.90	23.08

Plate Captions

Plate 1. Imaging sequence of 12 consecutive frames displaying global auroral activity at ultraviolet wavelengths in the interval 0719 - 0945 UT on 8 November 1981. Onset of a substorm occurs at ~ 0719 UT (first frame), with maximum epoch at ~ 0850 UT (eighth frame). The geocorona is visible in the scatterered light of solar Lyman-α radiation sunward of the dayside limb, at upper left in each frame. Antisunward of the terminator the entire auroral region is detected in the light of OI at 130.4 and 135.6 nm.

Plate 2. Smoothed Pedersen conductivity distribution for maximum epoch in the substorm overlayed on the image used to deduce the conductivity distribution. The maximum conductivity of ~ 32 mhos is located at ~ 63° latitude and ~ 0100 hours local time. The increment in conductivity between contours is 4 mhos. For the false-color image, light blue denotes emission intensities of ~ 2 kR, with greater intensities coded by green, yellow, red and white (> 32 kR). An eccentric-dipole-latitude, magnetic-local-time coordinate system is used. Concentric circles denote latitudes of 80°, 70°, 60° and 50°.

Plate 3. Modeled ionospheric current distribution at maximum epoch in the substorm overlayed on the image used to deduce the conductivity distribution (Plate 2). Peak ionospheric currents are ~ 1 A/m.

Plate 4. A continuation of Plate 3 for the modeled field-aligned current distribution. Solid lines denote contours for currents directed towards the ionosphere. Dashed lines denote contours for outward currents.

Figure Captions

Figure 1. Four ground and spacecraft investigations for studies of magnetospheric current systems. The three correlative investigations for observations at ground level and at near-earth distances are the subject of this work.

Figure 2. The spatial distribution of ground magnetometer stations at 0610 UT in an eccentric-dipole-latitude, magnetic-local-time format. The trajectory of DE 2 in the interval 0600 - 0620 UT on 7 November 1981 is mapped along the geomagnetic field to an altitude of 100 km.

Figure 3. Simultaneous observations of aurora and magnetic perturbations within the interval 0603:50 - 0607:10 UT on 7 November 1981 at ~ 0800 hours local time. Magnetic perturbations observed with the DE-2 spacecraft and the inferred field-aligned current densities are displayed in the upper and second panels, respectively. Model field-aligned currents deduced from magnetic perturbations observed at ground level are displayed in the third panel. The intensities of auroral OI emissions at 130.4 and 135.6 nm are presented in the lower panel.

Figure 4. A continuation of Figure 3 for the interval 0614:50 - 0619:10 UT at ~ 1800 hours local time.

Plate 1

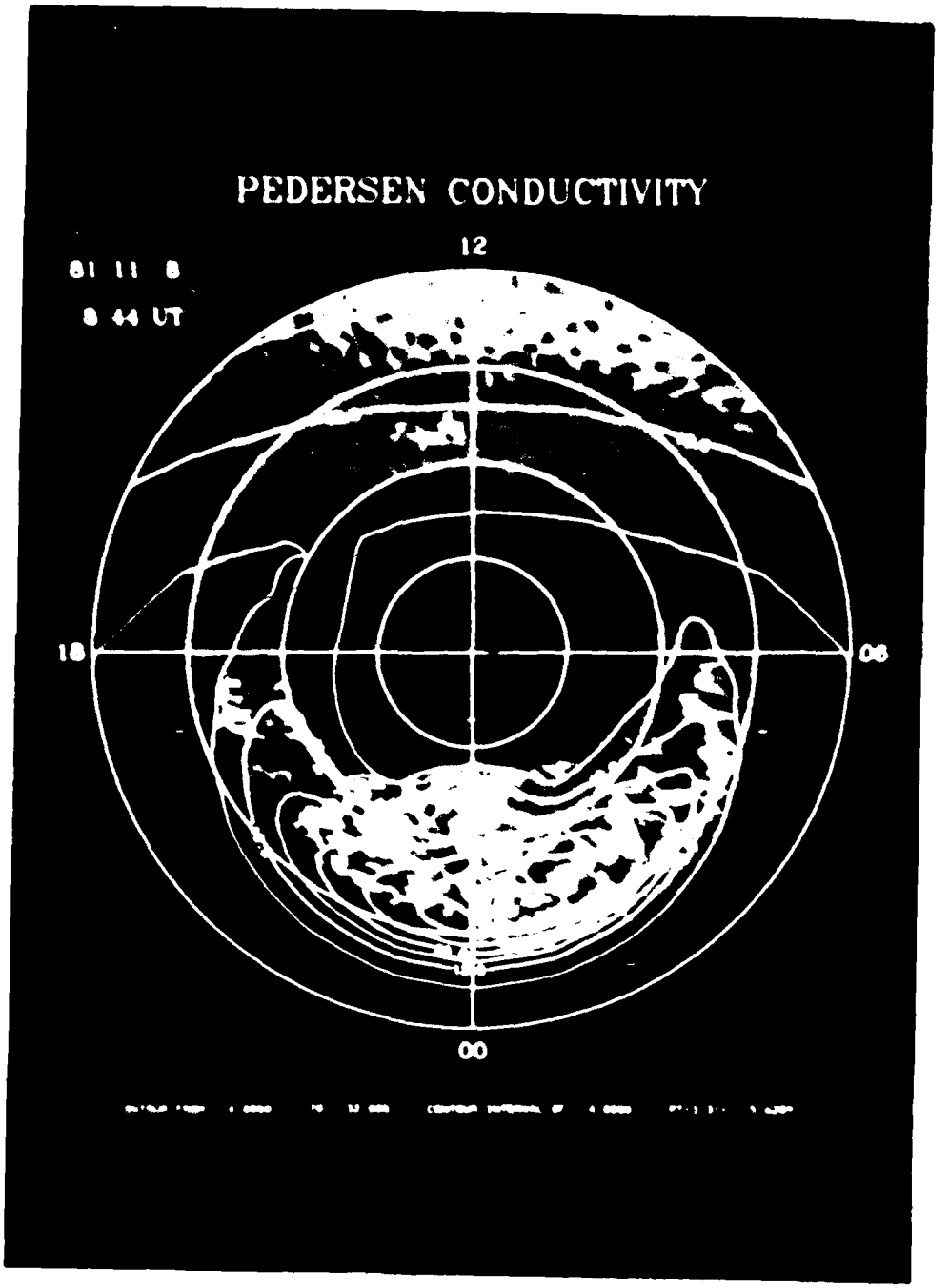

Plate 2

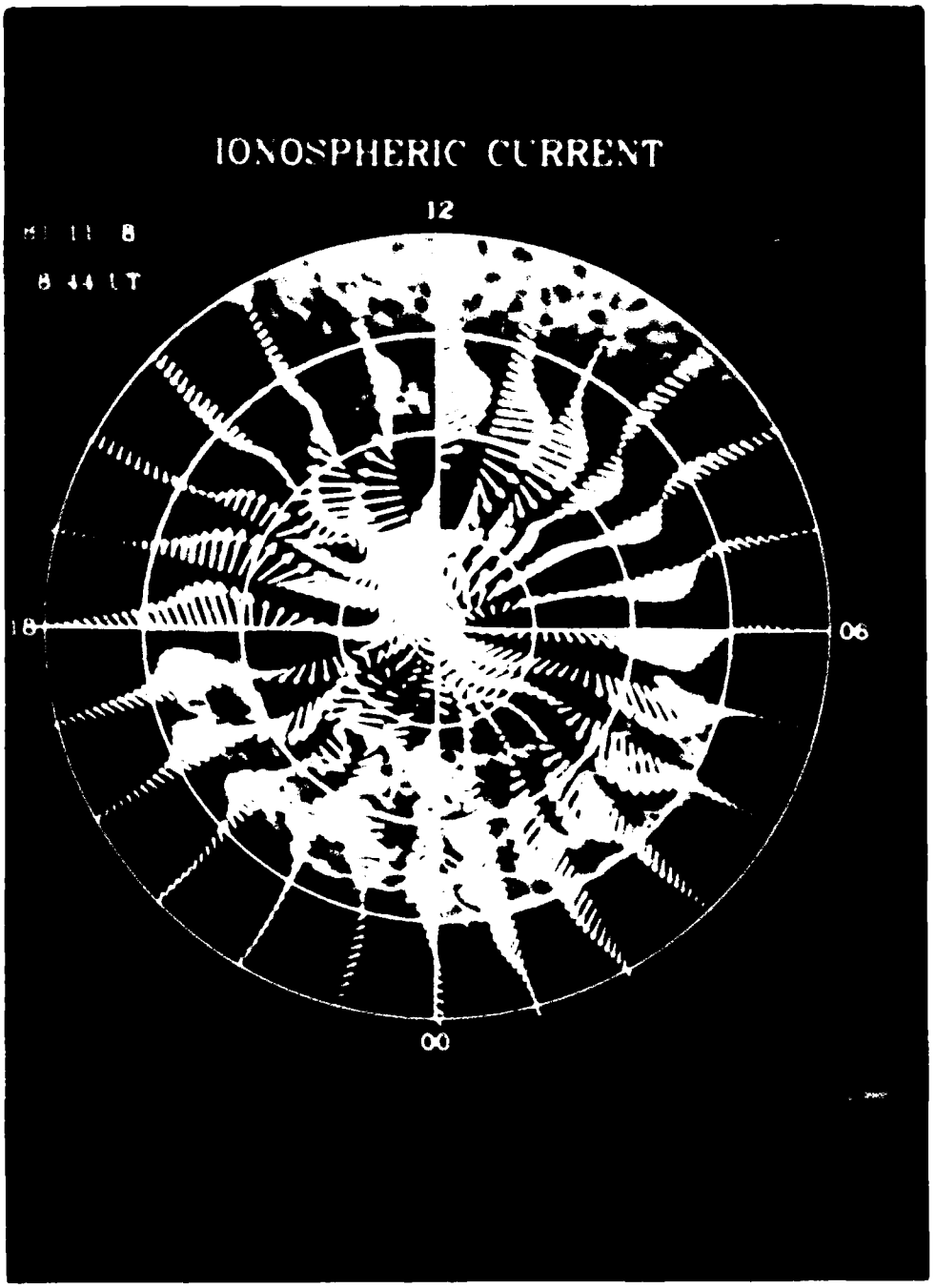

Plate 3

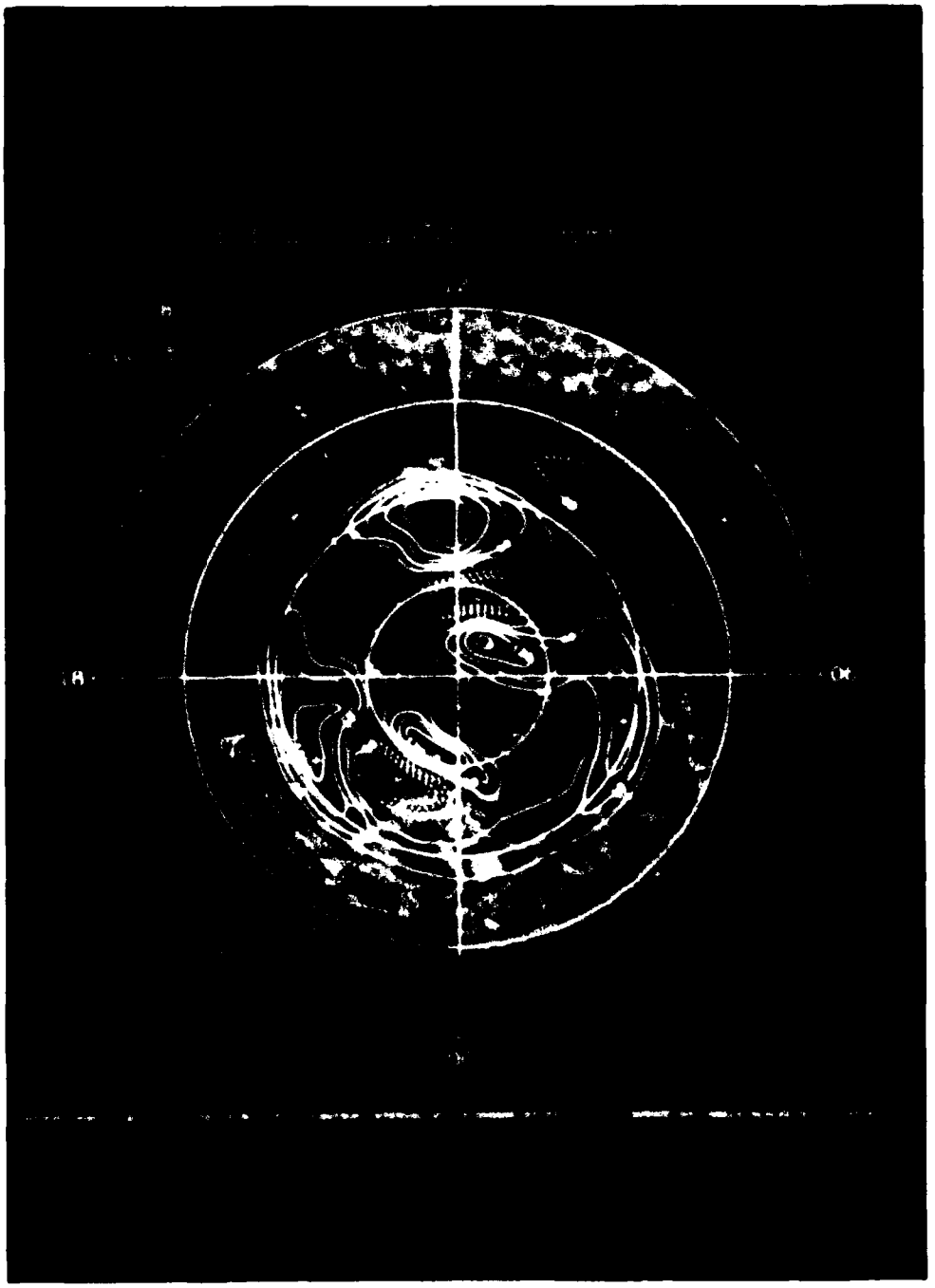

Plate 4

D-G83-254

SEVERAL CORRELATIVE INVESTIGATIONS OF MAGNETOSPHERIC CURRENT SYSTEMS

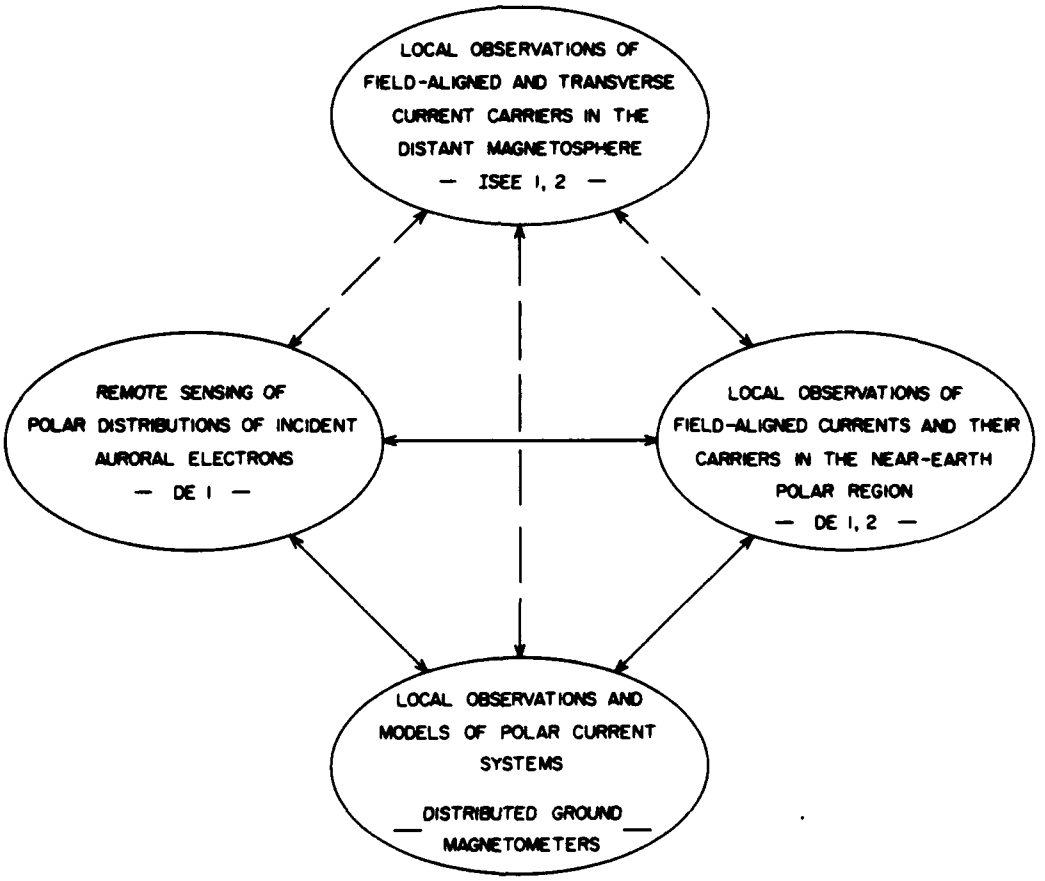

Figure 1

C-G83-253

LOCAL TIMES AND LATITUDES OF GROUND-BASED MAGNETOMETERS

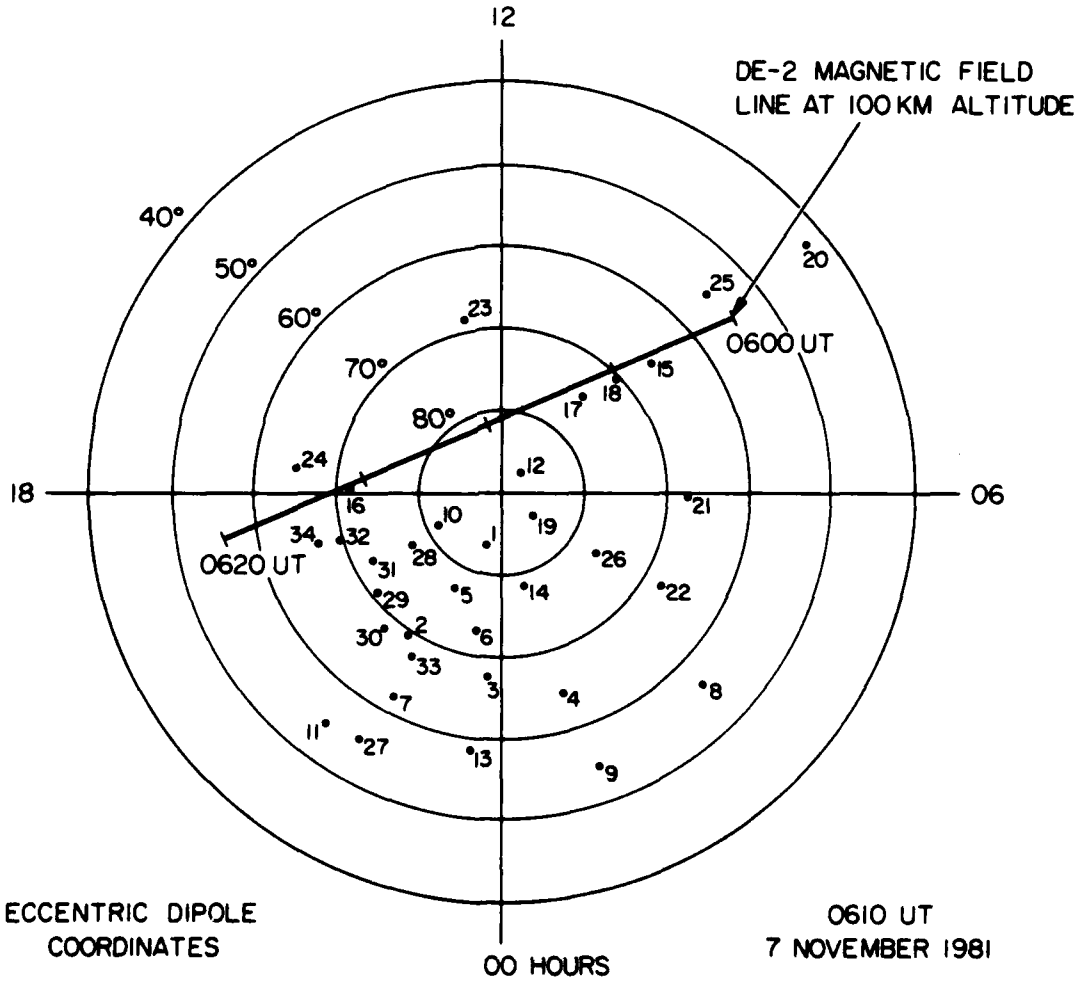

Figure 2

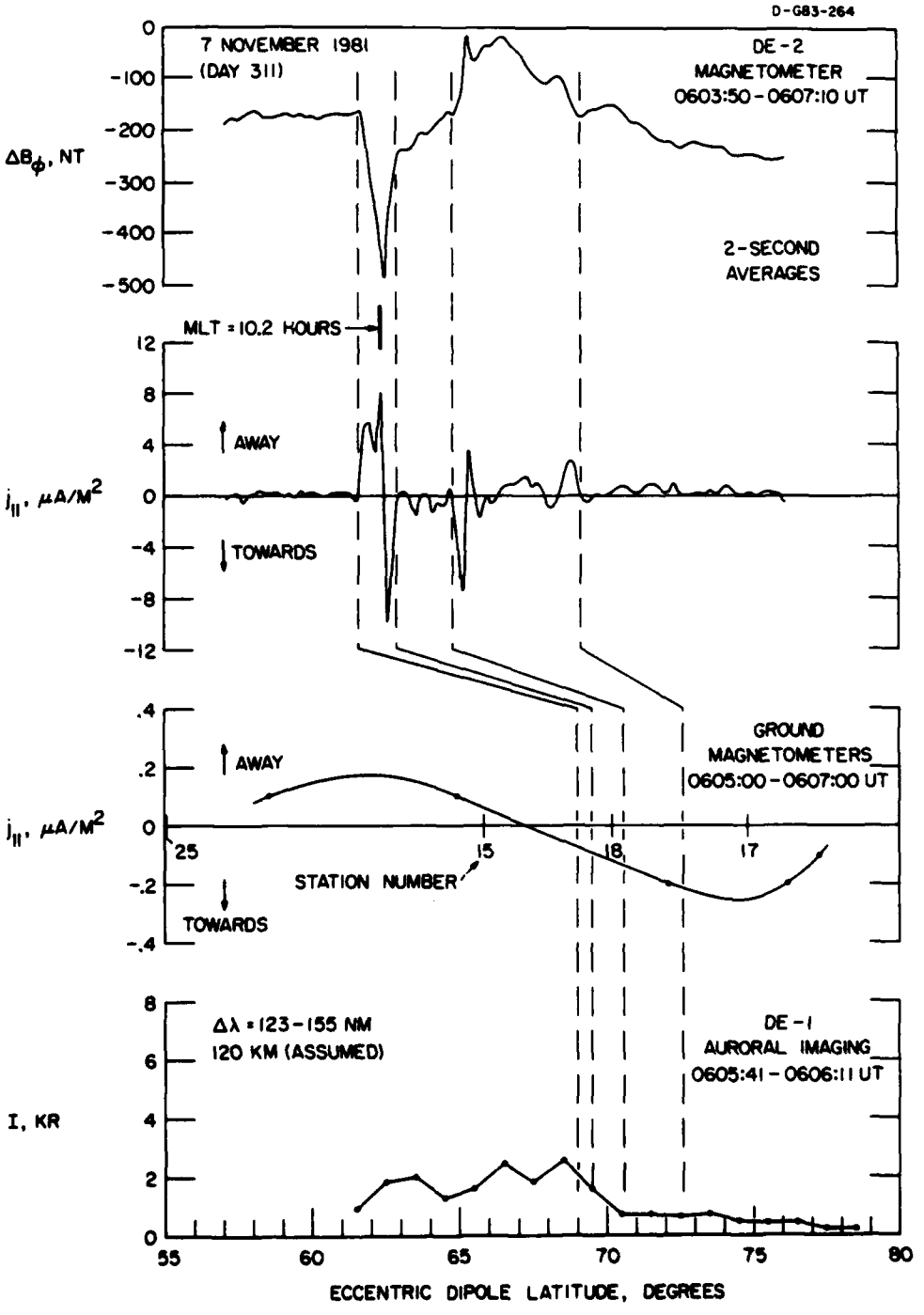
D-G83-264
7 NOVEMBER 1981
(DAY 311)
DE-2
MAGNETOMETER
0603:50 - 0607:10 UT
2-SECOND
AVERAGES
ΔB_ϕ, NT
0
-100
-200
-300
-400
-500
MLT = 10.2 HOURS
12
8
4
0
-4
-8
-12
AWAY
TOWARDS
$j_\parallel$, $\mu A/M^2$
GROUND
MAGNETOMETERS
0605:00 - 0607:00 UT
.4
.2
0
-.2
-.4
25
15
18
17
STATION NUMBER
$\Delta\lambda$ = 123 - 155 NM
120 KM (ASSUMED)
DE-1
AURORAL IMAGING
0605:41 - 0606:11 UT
I, KR
8
6
4
2
0
55
60
65
70
75
80
ECCENTRIC DIPOLE LATITUDE, DEGREES

Figure 3

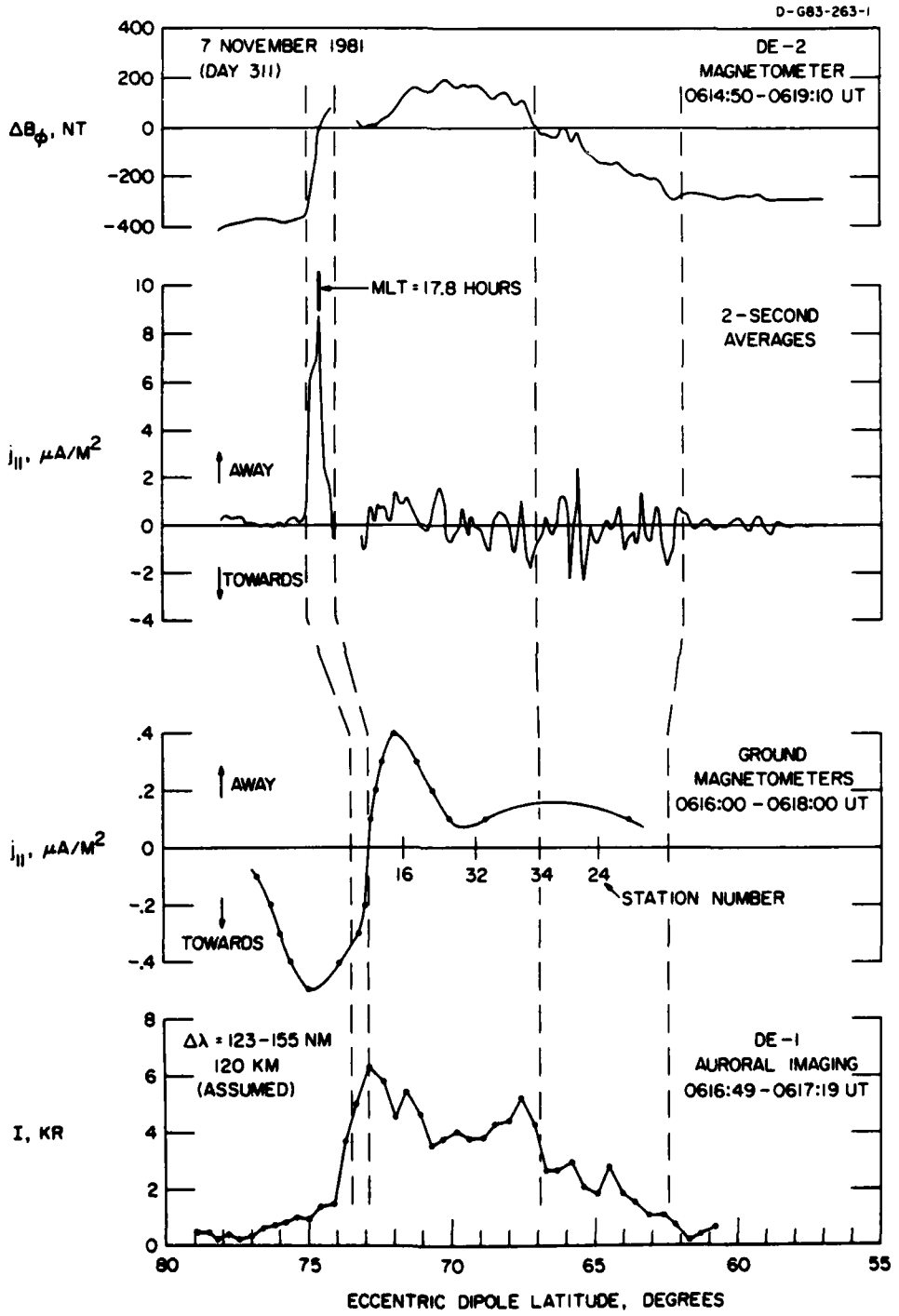
D-G83-263-1
7 NOVEMBER 1981
(DAY 311)
DE-2
MAGNETOMETER
0614:50-0619:10 UT
ΔB_ϕ, NT
400
200
0
-200
-400
MLT = 17.8 HOURS
2-SECOND
AVERAGES
$j_\parallel$, $\mu A/M^2$
10
8
6
4
2
0
-2
-4
AWAY
TOWARDS
GROUND
MAGNETOMETERS
0616:00-0618:00 UT
.4
.2
0
-.2
-.4
16
32
34
24
STATION NUMBER
$\Delta\lambda$ = 123-155 NM
120 KM
(ASSUMED)
DE-1
AURORAL IMAGING
0616:49-0617:19 UT
I, KR
8
6
4
2
0
80
75
70
65
60
55
ECCENTRIC DIPOLE LATITUDE, DEGREES

Figure 4

UNCLASSIFIED

SECURITY CLASSIFICATION OF THIS PAGE (When Data Entered)

REPORT DOCUMENTATION PAGE		READ INSTRUCTIONS BEFORE COMPLETING FORM
1. REPORT NUMBER U. of Iowa 83-26	2. GOVT ACCESSION NO. AD-A140615	3. RECIPIENT'S CATALOG NUMBER --
4. TITLE (and Subtitle) DISTRIBUTION OF AURORA AND IONOSPHERIC CURRENTS OBSERVED SIMULTANEOUSLY ON A GLOBAL SCALE		5. TYPE OF REPORT & PERIOD COVERED Scientific - 1981 6. PERFORMING ORG. REPORT NUMBER
7. AUTHOR(s) J. D. Craven, Y. Kamide, L. A. Frank, S.-I. Akasofu and M. Sugiura		8. CONTRACT OR GRANT NUMBER(s) N00014-76-C-0016
9. PERFORMING ORGANIZATION NAME AND ADDRESS Department of Physics and Astronomy University of Iowa Iowa City, Iowa 52242		10. PROGRAM ELEMENT, PROJECT, TASK AREA & WORK UNIT NUMBERS
11. CONTROLLING OFFICE NAME AND ADDRESS Office of Naval Research Electronic and Solid State Sciences Program Arlington, Virginia 22217		12. REPORT DATE August 1983 13. NUMBER OF PAGES 31
14. MONITORING AGENCY NAME & ADDRESS(if different from Controlling Office)		15. SECURITY CLASS. (of this report) UNCLASSIFIED 15a. DECLASSIFICATION/DOWNGRADING SCHEDULE

16. DISTRIBUTION STATEMENT (of this Report)

Approved for public release; distribution unlimited.

17. DISTRIBUTION STATEMENT (of the abstract entered in Block 20, if different from Report)

18. SUPPLEMENTARY NOTES

To be published in Magnetospheric Currents, AGU Monograph #28

19. KEY WORDS (Continue on reverse side if necessary and identify by block number)

AURORA, IONOSPHERIC CURRENTS, FIELD-ALIGNED CURRENTS

20. ABSTRACT (Continue on reverse side if necessary and identify by block number)

(See page following)

DD FORM 1 JAN 73 1473 EDITION OF 1 NOV 65 IS OBSOLETE
S/N 0102-LF-014-6601

UNCLASSIFIED
SECURITY CLASSIFICATION OF THIS PAGE (When Data Entered)

The instantaneous spatial distribution of auroral emissions is observed with auroral imaging photometers on board the spacecraft Dynamics Explorer 1 (DE 1) as ground-based meridian chains of magnetometers simultaneously detect the magnetic signatures of ionospheric and field-aligned currents flowing at northern polar latitudes. Ionospheric conductivities at nighttime auroral latitudes are estimated from the measured auroral luminosities and used with the measured polar magnetic variations to compute model distributions of ionospheric and field-aligned currents. Temporal resolution for the coordinated observations and model calculations is 12 minutes. Model ionospheric and field-aligned current distributions are overlayed on global auroral images to illustrate spatial relations on a global scale at the maximum epoch of an auroral substorm. Eccentric-dipole-latitude and magnetic-local-time coordinates are used. A model field-aligned current distribution is compared quantitatively with the distribution of field-aligned currents inferred from simultaneous observations by the DE-2 magnetometer.


DAT
FILM